

g -factor anisotropy in a GaAs/Al_xGa_{1-x}As quantum well probed by electron spin resonanceYu. A. Nefyodov,¹ A. V. Shchepetilnikov,¹ I. V. Kukushkin,¹ W. Dietsche,² and S. Schmult²¹*Institute of Solid State Physics RAS, 142432 Chernogolovka, Moscow District, Russia*²*Max-Planck-Institut für Festkörperforschung, Heisenbergstr. 1, 70569 Stuttgart, Germany*

(Received 9 December 2010; published 31 January 2011)

The anisotropy of electron g -factor is investigated for several GaAs/Al_xGa_{1-x}As heterostructures using an electrically detected electron spin resonance technique at liquid helium temperature. For a modulation-doped 25-nm single quantum well with electron density $n = 4 \times 10^{11} \text{ cm}^{-2}$ we extracted an out-of-plane g -factor value of $|g_{zz}| = 0.410$ and in-plane values of $|g_{yy}| = 0.359$ and $|g_{xx}| = 0.289$. In addition, linear in magnetic field corrections to the g -factor components were also extracted and strong anisotropy in their values was established.

DOI: [10.1103/PhysRevB.83.041307](https://doi.org/10.1103/PhysRevB.83.041307)

PACS number(s): 73.43.Lp, 73.43.Qt, 76.30.-v

The energy of the electron spin splitting, generally described by the g -factor tensor, in the case of bulk GaAs is reduced to a scalar, which is independent of the orientation of the magnetic field. The situation changes for the case of low-dimensional electron systems created in GaAs/Al_xGa_{1-x}As heterostructures. For example, in symmetric quantum wells grown along the crystallographic direction [001] the components of the g factor perpendicular to the two-dimensional (2D) plane, g_{zz} , and parallel to this plane, g_{xx} and g_{yy} , are not equal to each other.¹ However, in such symmetric quantum wells that have the point group $D2d$, the g factor of the electrons must be independent of the orientation of the parallel component of the magnetic field and, thus, $g_{xx} = g_{yy}$. On the contrary, in the case of an inversion-asymmetric quantum well (e.g., single-side-doped quantum well) whose point group is reduced to $C2v$, there are no more symmetry requirements forcing the g factor to be independent of the magnetic field orientation in the 2D plane. Moreover, such effects were calculated theoretically² and investigated experimentally.³ However, the experimentally established g -factor anisotropy in the 2D plane was found to be much smaller (about 10 times) than theoretically predicted. Note that most experimental works related to the measurements of g -factor components were based on optical quantum beating spectroscopy⁴ or time-resolved Kerr rotation,⁵ both having rather restricted precision, so that even a nonlinear magnetic field dependence of the Zeeman splitting was not detected by such methods. In addition, in optical detection schemes, a contribution from excitonic effects can easily mask properties of electron spin-splitting; in particular, they can average out anisotropy features.

In a previous Letter,⁶ we have shown that an electron spin linewidth (ESR) linewidth in samples with high electron mobility can be as narrow as 7 mT, corresponding to a spin relaxation time of ~ 10 ns. Mutual scattering of spin excitons appears to be the main relaxation mechanism for the case of filling factors close to $\nu = 1$. In the present work we employed a precise experimental transport technique⁷ based on direct measurements of electron spin resonance from high-quality electron systems. Due to a small ESR linewidth we were able to measure not only the components of the g -factor tensor (g_{xx} , g_{yy} , and g_{zz}), but also the correction terms describing the magnetic field dependence of the electronic g factor.

Three samples were studied. Sample 1 was a delta-silicon-doped Al_xGa_{1-x}As/GaAs heterojunction with the growth

direction [001]. The two-dimensional electron gas (2DEG) density was $1.35 \times 10^{11} \text{ cm}^{-2}$, whereas the mobility amounted to $3 \times 10^6 \text{ cm}^2/\text{V s}$ at liquid-helium temperature. The other two samples studied were asymmetrically doped 25-nm GaAs/Al_xGa_{1-x}As single quantum wells. The layers were grown by molecular-beam epitaxy on the [001] face of a GaAs wafer. Sample 2 had 2DEG density $4 \times 10^{11} \text{ cm}^{-2}$, whereas the mobility amounted to $10^6 \text{ cm}^2/\text{V s}$. Sample 3 was prepared from the similar wafer but had slightly different parameters, namely, $n = 3.6 \times 10^{11} \text{ cm}^{-2}$ and $\mu = 0.7 \times 10^6 \text{ cm}^2/\text{V s}$.

Due to the low number of spins, the conventional ESR technique cannot be successfully applied to a 2DEG.⁸ However, as early as 1983, Stein, von Klitzing, and Weimann⁹ showed the magnetoresistance of the 2DEG to be very sensitive to spin resonance, when the Fermi level is located between spin-split states of a given Landau level. To use this technique a usual Hall bar mesa was prepared with sides parallel to [110] and [1 $\bar{1}$ 0] directions. Further, we will refer to the in-plane directions parallel and perpendicular to the source-to-drain line as x and y , respectively. An ac probe current of $1 \mu\text{A}$ at the frequency of ~ 1 kHz was applied from source to drain. A lock-in amplifier monitored the channel resistance R_{xx} through two sense contacts along the channel. The sample was illuminated by 100% amplitude-modulated radiation at the frequency $f_{\text{mod}} \sim 30$ Hz; rf power was delivered from an Anritsu MG3696B generator through a rectangular waveguide. A second lock-in amplifier, synchronized at the frequency f_{mod} , was connected to the output of the first one and thus measured the change in the magnetoresistance δR_{xx} . In Fig. 1 we show typical ESR signals.

It is common knowledge that hyperfine interaction of electron and nuclear spins can cause dynamic polarization of nuclear spins, which results in shifting the position and changing the shape of the ESR line.^{10,11} The more the radiofrequency power, the more pronounced is this effect, which was successfully used to study nuclear spin relaxation rates.¹⁰ In our experiments, we used such low rf power that the influence of dynamic polarization was negligible, that is the ESR line shape and position did not change with rf power variations. The actual rf power incident to the sample amounted to $\lesssim 1$ mW. Experiments were carried out at temperatures of 1.3–4.2 K in magnetic fields up to 10 T. In our experiments, we fixed the microwave frequency and swept the magnetic field. In Ref. 6, we showed that the results of ESR measurements using frequency and magnetic field

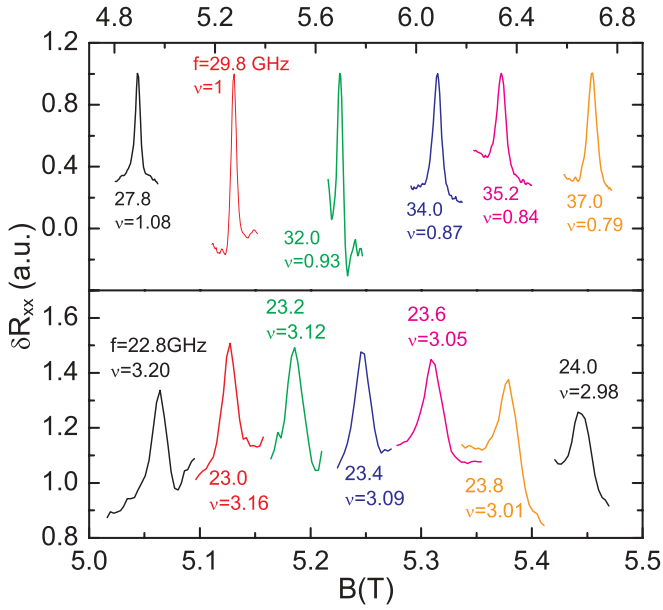


FIG. 1. (Color online) Examples of ESR resonance lines measured in a single heterojunction with $n = 1.35 \times 10^{11} \text{ cm}^{-2}$ near the filling factor $\nu = 1$ (upper panel) and in a 25-nm quantum well with $n = 4 \times 10^{11} \text{ cm}^{-2}$ near $\nu = 3$ (lower panel). The exact filling factor and microwave frequency values are shown for each line; the magnetic field is perpendicular to the 2DEG plane.

sweeps do coincide, but the magnetic field sweep is much more convenient.

The ESR signal was observed in the vicinity of filling factors $\nu = 3, 5, 7$ with the linewidth amounting to ~ 40 mT in this sample. In Fig. 2, the dependence of the ESR frequency on the magnetic field for the case of $\nu = 3$ is shown by solid squares.

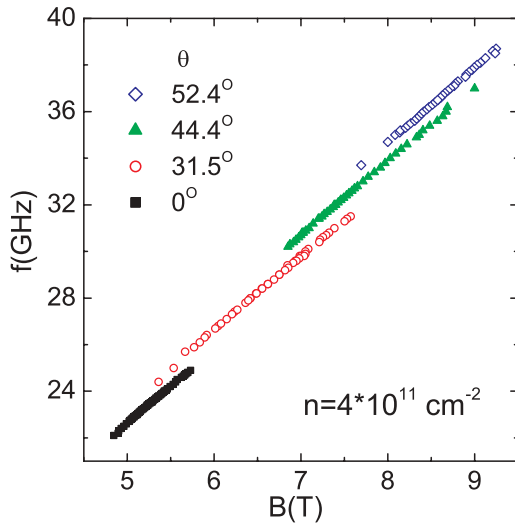


FIG. 2. (Color online) Dependences of ESR frequency on the magnetic field for four different values of angle θ between the magnetic field and the normal to the 2DEG plane. The experimental error is much smaller than the symbol size (the latter is about three times larger than the ESR linewidth and the microwave frequency is known to nine digits.)

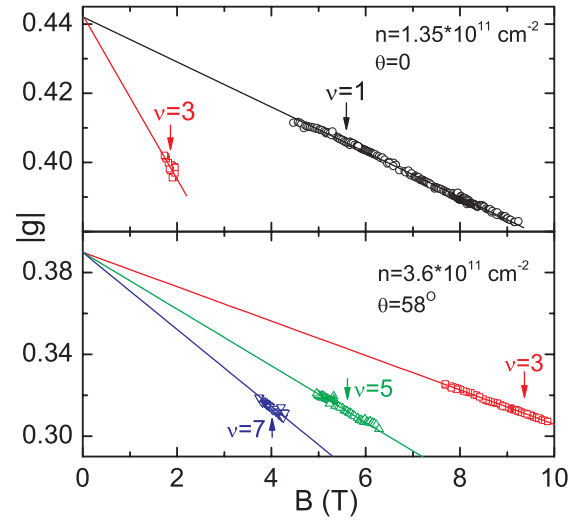


FIG. 3. (Color online) Magnetic field dependence of the g factor in a single heterojunction with $n = 1.35 \times 10^{11} \text{ cm}^{-2}$ (upper panel) and in a 25-nm quantum well with $n = 3.6 \times 10^{11} \text{ cm}^{-2}$ (lower panel).

From the magnetic field dependence of the ESR frequency shown in Fig. 2, one can extract the g -factor value and its dependence on the magnetic field. Note that in general one can represent the magnetic field dependence of the spin-splitting energy as a series:

$$E = E_s(0) + \mu_B g_i B_i + \gamma_i B_i^2 + \dots, \quad (1)$$

where $E_s(0)$ is the effective spin-splitting at zero magnetic field due to spin-orbit effects, g_i is the component of the g factor along the direction of the magnetic field B_i and γ_i is the component determining linear corrections to the g factor. First of all we extracted the value $E_s(0)$ using the most accurate measurements performed with sample 1 with the narrowest ESR line. The results are displayed in Fig. 3, where the magnetic field dependence of the g factor is shown over a wide range of the magnetic field, corresponding to filling factor variation from 1.25 to 0.6. Since we cannot extract the sign of the g factor, in all figures we show only its absolute value. It follows from the data in Fig. 3 that $E_s(0)/h = 0 \pm 0.4$ GHz and it means that we can neglect the first term in the series (1) and use a simpler formula to describe the magnetic field dependence of the g factor: $g_i(B) = g_i(0) + a_i B_i$. Such a dependence $g(B)$ was experimentally established for the case of perpendicular magnetic fields in Ref. 7 and theoretically explained¹² by taking into account nonparabolicity effects. As it follows from Fig. 3 a similar linear dependence of the g factor is also observed for the tilted magnetic field case. This justifies linear extrapolation of the g factor to zero magnetic field for any $\nu = 1, 3, 5$, which gives us the g factor for the subband bottom.

In order to study the g -factor anisotropy, we tilted the sample by the angle θ between the magnetic field and the normal to the 2DEG. Since the $R_{xx}(B)$ minimum is sensitive to the magnetic field component perpendicular to the 2DEG, this procedure shifts the range in which the ESR can be observed to higher magnetic fields and frequencies. Thus the measured g factor is a mixture of the components g_{zz} along the normal

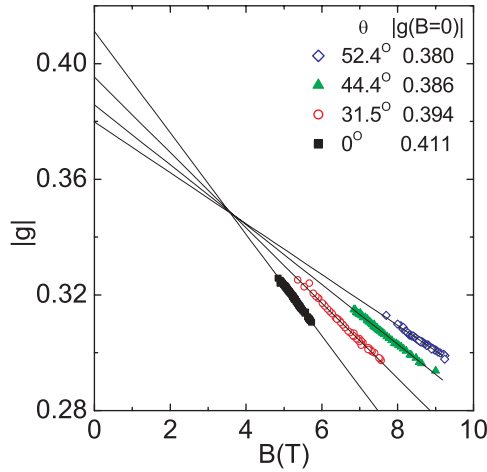


FIG. 4. (Color online) Dependences of the g factor on the magnetic field for four different values of the tilt angle θ between the magnetic field and the normal to the 2DEG plane. The values for the g factors shown are obtained by linear extrapolations of experimental data to zero magnetic field (lines).

to the 2DEG and the g_{yy} in-plane component according to the common formula $g_*^2 = g_{zz}^2 \cos^2 \theta + g_{yy}^2 \sin^2 \theta$. In Fig. 2, the dependence of the ESR frequency on the magnetic field is shown for four different θ values between 0 and 52.4 degrees. The latter value is restricted by the maximum possible magnetic field of 9.5 T of the experimental setup used.

The data sets in Fig. 2 do not form a continuous line, suggesting different g -factor values for each set. This becomes more apparent in Fig. 4, where g -factor values calculated from the previous graph are shown as a function of the magnetic field. The values of the effective g -factor linear extrapolations $g_*|_{B \rightarrow 0}$ to zero magnetic field are indicated in the upper right corner of Fig. 4. To obtain g_{yy} value according to Eq. (1) these zero field extrapolations squared $(g_*|_{B \rightarrow 0})^2$ are shown as a function of $\cos^2 \theta$ in Fig. 5 by open circles. The data in Fig. 5 can be well fitted by a straight line, which gives us the value $g_{yy} = 0.359$.

To investigate the in-plane anisotropy of the g factor, we performed one more set of experiments. Namely, the sample was tilted in such a manner that the in-plane magnetic field was directed parallel to the x axis. In this case, using the relation $g_*^2 = g_{zz}^2 \cos^2 \theta + g_{xx}^2 \sin^2 \theta$, we extracted g_{xx} values shown in Fig. 5 by solid squares. The linear extrapolation of these experimental data to zero $\cos \theta$ gives the value $g_{xx} = 0.289$. Thus, the in-plane g -factor anisotropy appeared to be of the same order of magnitude as the one between the in-plane and out-of-plane values. The directions $[110]$ and $[1\bar{1}0]$ appeared to be principal directions of the g -factor tensor, that is, g_{xx} and g_{yy} values extracted are principle values. More detailed investigation on this topic will be published elsewhere. From the experimental data we extracted also the linear on magnetic field correction term to the g -factor tensor according to the following formula: $g_{ij}(B) = g_{ij}(0) + a_{ijk} B_k$. Note that theoretically,¹² only one diagonal component of the a tensor, namely a_{zzz} , is expected to be nonzero. In the experiment we found $a_{zzz} = -0.0175 \pm 0.0001 \text{ T}^{-1}$ and $a_{xxx} = 0 \pm 0.002 \text{ T}^{-1}$. At the same time the data corresponding to the y direction

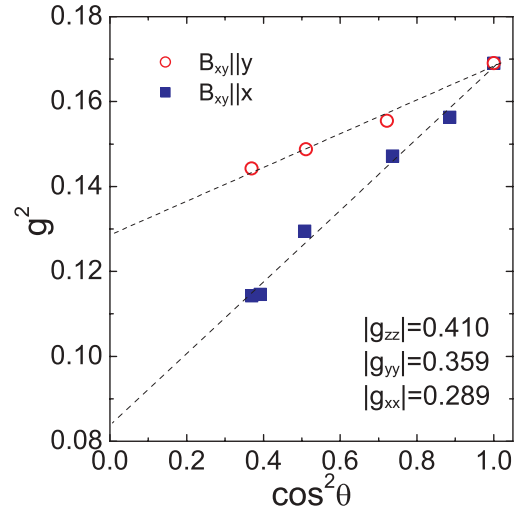


FIG. 5. (Color online) Squared g -factor values obtained by linear extrapolation to zero magnetic field vs $\cos^2 \theta$. Open circles and solid squares correspond to in-plane magnetic field directed along y and x axes, respectively.

can be well fitted using nonzero $a_{yyy} = -0.010 \pm 0.002 \text{ T}^{-1}$ or, even better, $a_{yyz} = -0.012 \pm 0.002 \text{ T}^{-1}$.

When we change the in-plane magnetic field orientation using the single Hall bar, we also change the angle between the probe current and in-plane magnetic field. A question arises of whether the in-plane g -factor anisotropy observed was due to change in the in-plane magnetic field orientation with respect to crystal axes or probe current. To verify this, we studied sample 3. Two Hall bar mesas, A and B , were prepared with source-to-drain lines parallel to the $[110]$ and $[1\bar{1}0]$ directions. Figure 6 shows the result of this experiment for the case of tilt angles $\theta = 0$ (squares) and $\theta = 58^\circ$ (circles and triangles for the cases of in-plane magnetic field B_{xy} directed along the y and x axes, respectively). Solid symbols were obtained

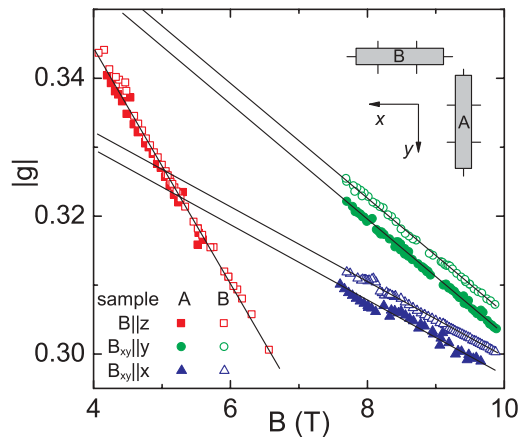


FIG. 6. (Color online) g -factor dependence on the magnetic field measured on the sample with two mesas (electron density is $n = 3.6 \times 10^{11} \text{ cm}^{-2}$). Solid and open symbols are for mesas A and B , respectively. Squares are the results for $B \parallel z$, whereas the rest of symbols are obtained for $\theta = 58^\circ$ (triangles and circles correspond to the cases of the in-plane magnetic field B_{xy} parallel to the x and y axes).

on mesa *A*, whereas open ones stand for mesa *B*. One can easily see that *g*-factor values for the in-plane magnetic field parallel to the *x* and *y* axes differ significantly, whereas the data sets obtained for the current flowing along two mutually perpendicular directions (mesas *A* and *B*) are parallel to each other and differ by not more than 1%. It should be noted also that the latter difference did not depend on the probe current value varied in the range $0.1 \div 10 \mu\text{A}$. This clearly indicates that the *g* factors measured depend only on the magnetic field orientation with respect to the crystal axes.

The presence of so-called wires at the sample surface could provide a possible explanation of the anisotropy observed. Ref. 13 shows high-mobility heterostructures produced by molecular beam epitaxy despite their purity to exhibit transport anisotropy, clearly seen especially in the fractional quantum Hall effect regime. This was unambiguously correlated to the presence of surface wires with the altitude scale of the order of 30 nm and seen through the aid of atomic-force microscopy (AFM). Another transport manifestation of wires is strong magnetoresistance anisotropy seen for various in-plane orientations of the magnetic field. We carefully

investigated our samples using both these techniques. AFM images demonstrated very smooth surface with absolutely random isotropic pattern and altitude variation amounting to 3 nm. Transport measurements did not reveal any anisotropy of the magnetoresistance in the parallel magnetic field either.

In conclusion, we experimentally found *g*-factor tensor diagonal components for a 25-nm-wide GaAs/Al_{*x*}Ga_{1-*x*}As single quantum well with 2D electron density $4 \times 10^{11} \text{ cm}^{-2}$ and the mobility amounted to $10^6 \text{ cm}^2/\text{V s}$. We clearly showed all three tensor components to be different, namely, out-of-plane $|g_{zz}| = 0.410$ and in-plane values are $|g_{yy}| = 0.359$ and $|g_{xx}| = 0.289$. Whereas the difference in the out-of-plane and in-plane values was theoretically predicted and experimentally confirmed, very strong in-plane anisotropy was experimentally found for the first time. Moreover, linear in magnetic field corrections to the *g*-factor components were also measured and strong anisotropy in their values was revealed.

The research was supported by Russian Foundation for Basic Research.

¹E. L. Ivchenko and A. A. Kiselev, *Sov. Phys. Semicond.* **26**, 827 (1992).

²V. K. Kalevich and V. L. Korenev, *Pis'ma Zh. Tekh. Fiz.* **57**, 557 (1993) [*JETP Lett.* **57**, 571 (1993)].

³S. Hallstein, M. Oestreich, W. W. Ruhle, and K. Kohler, *Proceedings of the 12th International Conference on the Application of High Magnetic Fields* (Wurzburg, Germany, 1996), p. 593.

⁴A. P. Heberle, W. W. Ruhle, and K. Ploog, *Phys. Rev. Lett.* **72**, 3887 (1994).

⁵A. Malinowski and R. T. Harley, *Phys. Rev. B* **62**, 2051 (2000).

⁶Yu. A. Nefyodov, A. A. Fortunatov, A. V. Shchepetilnikov, and I. V. Kukushkin, *Pis'ma Zh. Tekh. Fiz.* **91**, 385 (2010) [*JETP Lett.* **91**, 357 (2010)].

⁷M. Dohers, K. V. Klitzing, and G. Weimann, *Phys. Rev. B* **38**, 5453 (1988).

⁸N. Nestle, G. Denninger, M. Vidal, C. Weinzierl, K. Brunner, K. Eberl, and K. V. Klitzing, *Phys. Rev. B* **56**, R4359 (1997).

⁹D. Stein, K. V. Klitzing, and G. Weimann, *Phys. Rev. Lett.* **51**, 130 (1983).

¹⁰A. Berg, M. Dohers, P. R. Gerhardt, and K. von Klitzing, *Phys. Rev. Lett.* **64**, 2563 (1990).

¹¹E. Abrahams, *Physica E* **3**, 69 (1998).

¹²G. Lommer, F. Malcher, and U. Rössler, *Phys. Rev. B* **32**, 6965 (1985).

¹³R. L. Willett, J. W. P. Hsu, D. Natelson, K. W. West, L. N. Pfeiffer, *Phys. Rev. Lett.* **87**, 126803 (2001).